

# Probing Nano-Mechanical QED Effects

Y. B. Gao,<sup>1,2,\*</sup> S. Yang,<sup>1,3</sup> Yu-xi Liu,<sup>1,4</sup> C. P. Sun,<sup>1,3</sup> and Franco Nori<sup>1,4,5</sup>

<sup>1</sup>*Advanced Science Institute, The Institute of Physical and Chemical Research (RIKEN), Wako-shi 351-0198, Japan*

<sup>2</sup>*College of Applied Sciences, Beijing University of Technology, Beijing, 100124, China*

<sup>3</sup>*Institute of Theoretical Physics, The Chinese Academy of Sciences, Beijing, 100190, China*

<sup>4</sup>*CREST, Japan Science and Technology Agency (JST), Kawaguchi, Saitama 332-0012, Japan*

<sup>5</sup>*Center for Theoretical Physics, Physics Department, Center for the Study of Complex Systems, The University of Michigan, Ann Arbor, Michigan 48109-1040, USA*

(Dated: February 15, 2009)

We propose and study an “intrinsic probing” approach, without introducing any external detector, to mimic cavity QED effects in a qubit-nanomechanical resonator system. This metallic nanomechanical resonator can act as an intrinsic detector when a weak driving current passes through it. The nanomechanical resonator acts as both the cavity and the detector. A cavity QED-like effect is demonstrated by the correlation spectrum of the electromotive force between the two ends of the nanomechanical resonator. Using the quantum regression theorem and perturbation theory, we analytically calculate the correlation spectrum. In the weak driving limit, we study the effect on the vacuum Rabi splitting of both the strength of the driving as well as the frequency-detuning between the charge qubit and the nanomechanical resonator. Numerical calculations confirm the validity of our intrinsic probing approach.

PACS numbers: 85.85.+j, 85.25.Cp

## I. INTRODUCTION

Recently, nanomechanical resonators (NAMRs) are attracting considerable attention (see, e.g., Refs. 1, 2,3,4). Also, mechanical analogues of cavity QED have been theoretically studied in coupled systems between nanomechanical resonators and superconducting qubits (see, e.g., Refs. 5,6,7,8,9). Various effects in these nanomechanical QED systems were investigated, including: quantum measurements<sup>6</sup>, the quantum squeezing of the NAMRs<sup>9,10,11</sup>, and the cooling of the NAMRs<sup>12,13,14,15,16</sup>. Some of these theoretical proposals have recently become experimentally testable due to the recent advances in NAMRs and superconducting qubits. Numerous Josephson-junction-based superconducting qubits have been experimentally realized (see, e.g., the reviews<sup>17,18,19,20</sup>), while studies on NAMRs with vibration frequencies of the order of a GHz are approaching the quantum regime.

References<sup>21,22</sup> recently studied a NAMR coupled to a double-quantum dot. In Ref. 21, the spectrum of the transport current was used to study the quantum behavior of this system. The electron transport through a mobile island (i.e., a nanomechanical oscillator) with two energy levels was studied in Ref. 23. There, the qubit was embedded in the NAMR.

To study cavity QED analogues in a NAMR-qubit system, a crucial issue is how to make the quantum measurement on this coupled system. Quantum measurements involve subtle interactions between the system and the detector. To carry out a quantum measurement, an external probing instrument is typically coupled to the measured system. Examples of this include: a single electron transistor<sup>24</sup> coupled to a charge qubit, a transmission line resonator<sup>25,26,27</sup> coupled to a charge qubit,

or a shunted dc-SQUID coupled to a flux qubit (see, e.g., Refs. 28,29,30). In general, these coupled systems can be modeled by the Jaynes-Cummings Hamiltonian and demonstrate several analogues to cavity QED effects<sup>31,32</sup>, such as vacuum Rabi splitting. These effects can be used to verify the coherent coupling between a superconducting qubit and a measuring device.

This study is mainly motivated by recent experiments on a high-frequency metallic NAMR<sup>33</sup>. Previously, non-metallic NAMRs were often studied and therefore no efficient current would pass through these non-metallic NAMRs, and thus no mechanical force acting on the NAMRs could be induced to implement quantum measurements. In this case, an external instrument needs to be integrated to probe the coupling between the NAMR and the qubit. Here, we study how to probe a cavity QED analogue for a metallic NAMR<sup>33</sup> coupled to a superconducting qubit *without* introducing an external detector.

In this proposal, the information on the coherent coupling between the superconducting charge qubit and the metallic NAMR can be read out by measuring the induced electromotive force between the two ends of the NAMR. This electromotive force is generated by a current passing through a metallic NAMR in which a magnetic field is applied. There are at least two advantages for this intrinsic probing mechanism: (i) the coupling between the metallic NAMR and the qubit can be turned on or off by the externally-applied voltage, and then the information can be read out in a controllable way; (ii) no external probing instrument needs to be introduced, in contrast to the proposal in Ref. 34.

This paper is organized as follows. In Sec. II, we describe the proposed model, and write the Hamiltonian for a charge qubit interacting with a driven metallic NAMR. In Sec. III, we calculate the spectrum of the two-time

correlation function for the induced electromotive force using the quantum regression theorem<sup>35</sup> and perturbation theory. In the weak driving limit, we study how the Rabi splitting depends on both the strength of the driving current which passes through the NAMR as well as the detuning between the frequencies of the charge qubit and the nanomechanical resonator. Using numerical calculations, we demonstrate that our analytical results are valid in the weak driving limit. Finally, we summarize our conclusions.

## II. MODEL

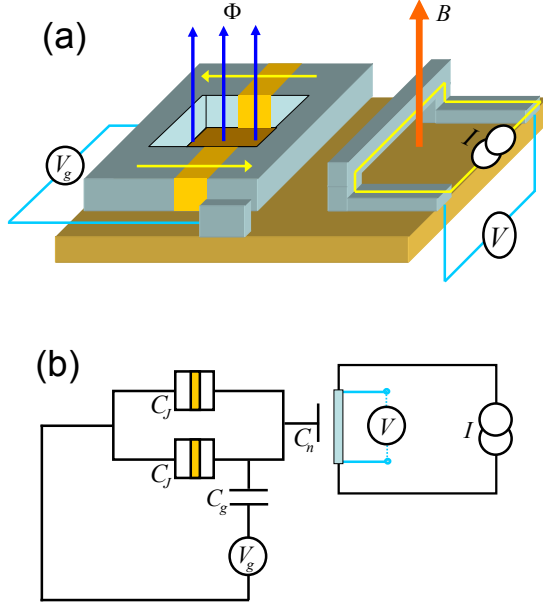


FIG. 1: (Color online) (a) Schematic diagram of a charge qubit (grey loop on the left) capacitively coupled to a metallic nanomechanical resonator (NAMR) shown on the right. An external ac current,  $I(t) = I_0 \sin(\omega_p t)$ , shown in yellow, passes through the NAMR. Also a magnetic field  $B$  (red line with the up arrow) is applied to the NAMR. The magnetic flux  $\Phi$  through the SQUID is denoted by the blue upward-pointing arrows. The induced electromotive force  $V$  (defined in Eq. (1)) at both ends of the NAMR can be used to detect information on the quantum-coherent coupling. A simple circuit diagram for (a) is given in (b). Here,  $C_J$  and  $C_g$  represent the capacitances for the Josephson junctions and the gate capacitor, respectively. Also,  $V_g$  is the gate voltage applied to the qubit via the gate capacitor.

As shown in Fig. 1, we study a metallic NAMR, which is capacitively coupled to a SQUID-based Cooper pair box (qubit). The distributed capacitance between the NAMR and the superconducting island of the qubit is denoted by  $C_n(x)$ . Here no voltage is applied to this

distributed capacitor, in contrast to previous work<sup>9</sup>. The electromagnetic force drives the NAMR to oscillate and the induced electromotive force between the two ends of the NAMR can be described by

$$V = Bl \frac{dx}{dt} = Bl \frac{p}{M}. \quad (1)$$

Here  $l$  and  $M$  denote the length and the mass of the NAMR, respectively. Also,  $(dx/dt) = (p/M)$  denotes the velocity of the NAMR;  $p$  represents the momentum for the center of mass of the NAMR;  $x$  denotes the small displacement of the NAMR around the coordinate-axis origin, and  $x = 0$  when no ac current passes through the NAMR. The Hamiltonian  $H_{\text{NAMR}}$  for the ac-current-driven NAMR is given by

$$H_{\text{NAMR}} = \frac{p^2}{2M} + \frac{1}{2}M\Omega^2 x^2 - lBI(t)x, \quad (2)$$

where the canonical coordinate  $x$  and momentum  $p$  for the NAMR are assumed to satisfy the commutation relation  $[x, p] = i$ . Hereafter, we assume  $\hbar = 1$ . The parameter  $\Omega$  denotes the oscillating frequency of the NAMR. The  $x$  and  $p$  of the NAMR can be represented by the annihilation  $a$  and creation  $a^\dagger$  operators as,

$$x = \frac{1}{\sqrt{2M\Omega}} (a^\dagger + a), \quad (3)$$

$$p = i\sqrt{\frac{M\Omega}{2}} (a^\dagger - a). \quad (4)$$

Thus the Hamiltonian in Eq. (2) can be rewritten as

$$H_{\text{NAMR}} = \Omega a^\dagger a - \frac{lB}{\sqrt{2M\Omega}} (a + a^\dagger) I(t). \quad (5)$$

Let us now assume that the SQUID has two identical Josephson junctions, each with the Josephson energy  $E_{J0}$  and capacitance  $C_J$ . A control gate voltage  $V_g$  is applied to the Cooper-pair box via the gate capacitor with the capacitance  $C_g$ . The Hamiltonian of the box can be written<sup>18,20,36</sup> as

$$H_c = \frac{2e^2}{C_\Sigma(x)} (n - n_g)^2 + E_J \cos \varphi \quad (6)$$

with the controllable effective Josephson energy  $E_J = 2E_{J0} \cos(\pi\Phi/\Phi_0)$  of the SQUID. Here,  $\Phi$  is the magnetic flux through the SQUID loop and  $\Phi_0$  is the flux quantum. The total capacitance  $C_\Sigma(x)$  connected to the superconducting island is given by

$$C_\Sigma(x) = 2C_J + C_g + C_n(x).$$

The effective Cooper pair number  $n_g$  in the superconducting island is  $n_g = C_g V_g / (2e)$ . We assume that the distance  $d$  between the NAMR and the superconducting island is much larger than the amplitude  $x$  of the oscillation of the NAMR, i.e.,  $d \gg x$ . In this case, the distributed capacitance can be approximately written as

$$C_n(x) \simeq C_n \left(1 - \frac{x}{d}\right) \quad (7)$$

to first order in  $x/d$ . The island's charging energy is  $E_C = e^2/[2C_\Sigma(0)]$  and  $n_g$  is near the degeneracy point  $1/2$ . In these conditions, the box can be reduced to a two-level quantum system and the Hamiltonian in Eq. (6) can be reduced to

$$H_c = 4E_C \left( n_g - \frac{1}{2} \right) \left( 1 + \frac{C_n}{C_\Sigma(0)} \frac{x}{d} \right) \bar{\sigma}_z - \frac{1}{2} E_J \bar{\sigma}_x \quad (8)$$

in spin-1/2 notation with the quasi-spin operators

$$\begin{aligned} \bar{\sigma}_z &= |0\rangle_{cc} \langle 0| - |1\rangle_{cc} \langle 1|, \\ \bar{\sigma}_x &= |0\rangle_{cc} \langle 1| + |1\rangle_{cc} \langle 0|, \end{aligned}$$

which are defined in the basis of the charge states  $|0\rangle_c$  and  $|1\rangle_c$ . Equation (8) is used to describe the interaction between the NAMR and the charge qubit.

We now reconstruct a set of spin operators  $\{\sigma_z, \sigma_\pm\}$  with

$$\sigma_+ |0\rangle = |1\rangle, \quad \sigma_- |1\rangle = |0\rangle, \quad (9)$$

and

$$|1\rangle = \cos \frac{\theta}{2} |0\rangle_c - \sin \frac{\theta}{2} |1\rangle_c, \quad (10)$$

$$|0\rangle = \sin \frac{\theta}{2} |0\rangle_c + \cos \frac{\theta}{2} |1\rangle_c, \quad (11)$$

where the mixing angle  $\theta$  is determined by

$$\tan \theta = \frac{E_J}{4E_C (2n_g - 1)}.$$

In the new basis  $|0\rangle$  and  $|1\rangle$ , the Hamiltonian in Eq. (8) becomes

$$H_c = \frac{\omega_a}{2} \sigma_z + \frac{4E_C C_n}{dC_\Sigma(0)} \left( n_g - \frac{1}{2} \right) (\cos \theta \sigma_z + \sin \theta \sigma_x) x \quad (12)$$

with the qubit frequency

$$\omega_a = \sqrt{16E_C^2 (2n_g - 1)^2 + E_J^2}. \quad (13)$$

Notice that the coupling between the coordinate  $x$  of the NAMR and the qubit has a term proportional to the gate voltage ( $\propto n_g$ ). Thus, the gate voltage  $V_g$  can control this coupling. Using Eq. (12) and also considering the driven NAMR, we can now write down the total Hamiltonian of the driven NAMR interacting with the charge qubit

$$H = H_c + H_{\text{NAMR}}. \quad (14)$$

Here, the Hamiltonians  $H_{\text{NAMR}}$  and  $H_c$  are given by Eqs. (5) and (12), respectively.

In the rotating reference frame at the driven frequency  $\omega_p$ , for both the qubit and the NAMR, through the unitary transformation

$$U = \exp \left[ -i\omega_p \left( \frac{1}{2} \sigma_z - a^\dagger a \right) t \right], \quad (15)$$

the total Hamiltonian in Eq. (14) is converted into an effective time-independent Hamiltonian

$$H_{\text{eff}} = \Delta_a \sigma_+ \sigma_- + g (a \sigma_+ + a^\dagger \sigma_-) + \Delta a^\dagger a - \xi (a + a^\dagger). \quad (16)$$

Here, the fast oscillating terms  $\exp(i\omega_d t)$  and  $\exp(2i\omega_d t)$  have been neglected, and we also used the identity,  $\sigma_z = 2\sigma_+ \sigma_- - I$ , where  $I$  is the unit operator. In Eq. (16), the detuning  $\Delta_a$  between the frequencies of the qubit and the ac driving current is

$$\Delta_a \equiv \Delta_{\text{qubit-current}} = \omega_a - \omega_p. \quad (17)$$

The detuning  $\Delta$  between the frequencies of the NAMR and the ac driving current is

$$\Delta \equiv \Delta_{\text{NAMR-current}} = \Omega - \omega_p. \quad (18)$$

The interaction strength  $g$  (between the qubit and the NAMR) is

$$g \equiv g_{\text{qubit-NAMR}} = \left( n_g - \frac{1}{2} \right) \frac{1}{\sqrt{2M\Omega}} \frac{4E_C C_n}{dC_\Sigma(0)} \sin \theta,$$

which can be switched off when  $n_g = 1/2$ . The coupling strength (between the NAMR and the ac driving current) is

$$\xi \equiv \xi_{\text{NAMR-current}} = \frac{lBI_0}{2} \frac{1}{\sqrt{2M\Omega}}. \quad (19)$$

Note that the coupling  $g$  is proportional to the gate voltage, while the other coupling strength  $\xi$  is proportional to  $BI_0$ .

### III. CORRELATION SPECTRUM OF THE INDUCED ELECTROMOTIVE FORCE

The first three terms of the right hand side of  $H_{\text{eff}}$  in Eq. (16) describe the Jaynes-Cummings Hamiltonian, which was extensively studied in cavity QED. This QED analogue of the qubit-NAMR, described in Eq. (16), can be studied via the correlation spectrum  $S_V(\omega)$  of the induced electromotive force

$$V = iBl \sqrt{\frac{\Omega}{2M}} (a^\dagger - a), \quad (20)$$

which is obtained from Eq. (1) by replacing the momentum operator  $p$  with Eq. (4). The correlation spectrum  $S_V(\omega)$  of the induced electromotive force  $V$  can be calculated via

$$S_V(\omega) = \frac{1}{\pi} \text{Re} \int_0^\infty d\tau e^{i\omega\tau} \langle V(0)V(\tau) \rangle. \quad (21)$$

Equation (20) shows that the two-time correlation function  $\langle V(0)V(\tau) \rangle$  in Eq. (21) can be calculated as

$$\begin{aligned} \langle V(0)V(\tau) \rangle &\propto \langle a(0)a^\dagger(\tau) \rangle + \langle a^\dagger(0)a(\tau) \rangle \\ &\quad - \langle a(0)a(\tau) \rangle - \langle a^\dagger(0)a^\dagger(\tau) \rangle. \end{aligned} \quad (22)$$

### A. Master equation and solutions

To obtain the correlation spectrum, we start from the master equation<sup>37</sup> of the reduced density matrix  $\rho$  for the qubit-NAMR system

$$\dot{\rho} = -i[H_{\text{eff}}, \rho] + \kappa(2a\rho a^\dagger - a^\dagger a\rho - \rho a^\dagger a) + \frac{\gamma}{2}(2\sigma_- \rho \sigma_+ - \sigma_+ \sigma_- \rho - \rho \sigma_+ \sigma_-), \quad (23)$$

where the latter two terms describe the decays of the NAMR and the charge qubit, respectively. The parameters  $\kappa$  and  $\gamma$  denote the decay rates of the NAMR and the qubit, respectively. We also use the Markov approximation when Eq. (23) is derived. For convenience below, we now define the number operator,  $N = \sigma_+ \sigma_- + a^\dagger a$ , to characterize the total excitation of the qubit-NAMR. Obviously,  $N$  satisfies

$$N|j, k\rangle = (j+k)|j, k\rangle.$$

Here, the index  $j$  represents the states of the charge qubit. When the qubit is in an excited state, we take  $j = 1$ , otherwise  $j = 0$ . Also  $k$  denotes the phonon number of the oscillating NAMR, i.e.,  $a^\dagger a|k\rangle = k|k\rangle$ .

We are only interested in the weak driving limit, i.e.,

$$\xi \equiv \xi_{\text{NAMR-current}} \rightarrow 0.$$

In this limit, we only need to consider the zero- and one-particle excitations; then  $N$  satisfies the condition

$$N = j + k = 0, 1. \quad (24)$$

The Hilbert space for the reduced density matrix is now limited to a smaller subspace with a truncated basis

$$\{|j, k\rangle, j + k = 0, 1\}. \quad (25)$$

Therefore, in this truncated basis, the density matrix elements satisfy the following equations

$$\begin{aligned} \frac{d\rho_{00,00}}{d\tau} &= i\xi\rho_{01,00} - i\xi\rho_{00,01} + 2\kappa\rho_{01,01} + \gamma\rho_{10,10}, \\ \frac{d\rho_{00,01}}{d\tau} &= (i\Delta - \kappa)\rho_{00,01} + ig\rho_{00,10} \\ &\quad + i\xi(\rho_{01,01} - \rho_{00,00}), \\ \frac{d\rho_{00,10}}{d\tau} &= \left(i\Delta_a - \frac{\gamma}{2}\right)\rho_{00,10} + ig\rho_{00,01} + i\xi\rho_{01,10}, \\ \frac{d\rho_{01,01}}{d\tau} &= -2\kappa\rho_{01,01} + ig(\rho_{01,10} - \rho_{10,01}) \\ &\quad + i\xi(\rho_{00,01} - \rho_{01,00}), \\ \frac{d\rho_{01,10}}{d\tau} &= \left(i\Delta_a - i\Delta - \kappa - \frac{\gamma}{2}\right)\rho_{01,10} \\ &\quad + ig(\rho_{01,01} - \rho_{10,10}) + i\xi\rho_{00,10}, \\ \frac{d\rho_{10,10}}{d\tau} &= -\gamma\rho_{10,10} + ig(\rho_{10,01} - \rho_{01,10}). \end{aligned} \quad (26)$$

The other non-diagonal matrix elements  $\rho_{01,00}(\tau)$ ,  $\rho_{10,00}(\tau)$ , and  $\rho_{10,01}(\tau)$  can be easily obtained by taking the complex conjugates of  $\rho_{00,01}(\tau)$ ,  $\rho_{00,10}(\tau)$ , and

$\rho_{01,10}(\tau)$ , e.g.,  $\rho_{01,00}(\tau) = [\rho_{00,01}(\tau)]^*$  when their solutions, e.g.,  $\rho_{00,01}(\tau)$ , are obtained using Eq. (26).

In the weak driving limit,  $\xi \ll g$ , we take the population in the ground state as  $\rho_{00,00} = 1$ . We also find that two diagonal matrix elements ( $\rho_{10,10}$  and  $\rho_{01,01}$ ) and two off-diagonal matrix elements ( $\rho_{01,10}$  and  $\rho_{10,01}$ ) are proportional to  $\xi^2$ . The other ones are proportional to  $\xi$ . Using perturbation theory, we only keep the terms to first order in  $\xi$  for the reduced matrix elements in Eq. (26) and then we can obtain

$$\dot{\rho}_{00,01} = (i\Delta - \kappa)\rho_{00,01} + ig\rho_{00,10} - i\xi, \quad (27)$$

$$\dot{\rho}_{00,10} = \left(i\Delta_a - \frac{\gamma}{2}\right)\rho_{00,10} + ig\rho_{00,01}. \quad (28)$$

Applying the Laplace transformation to Eq. (27) and Eq. (28), the solutions of the matrix element  $\rho_{00,01}(\tau)$  can be easily obtained as

$$\rho_{00,01}(\tau) = \eta_{12}e^{-\lambda_1\tau} + \eta_{21}e^{-\lambda_2\tau} + \varepsilon, \quad (29)$$

with parameters

$$\varepsilon = \frac{i\xi(i\Delta_a - \frac{\gamma}{2})}{\lambda_1\lambda_2},$$

$$\eta_{mn} = \mu_{mn}\rho_{00,01}(0) + \chi_{mn}\rho_{00,10}(0) + i\xi\nu_{mn}.$$

Other parameters  $\mu_{mn}$ ,  $\chi_{mn}$ ,  $\nu_{mn}$ ,  $\lambda_1$ , and  $\lambda_2$  in Eq. (29) are

$$\begin{aligned} \mu_{mn} &= \frac{\lambda_m + (i\Delta_a - \frac{\gamma}{2})}{(\lambda_m - \lambda_n)}, \\ \chi_{mn} &= \frac{\lambda_m + (i\Delta_a - \frac{\gamma}{2})}{\lambda_m(\lambda_m - \lambda_n)}, \\ \nu_{mn} &= \frac{g}{i(\lambda_m - \lambda_n)}, \end{aligned} \quad (30)$$

and

$$\lambda_m = \Gamma + \frac{i}{2} \left[ (-1)^m \sqrt{\left(\delta - i\left(\kappa - \frac{\gamma}{2}\right)\right)^2 + 4g^2} - (\Delta_a + \Delta) \right].$$

for  $m(\neq n) = 1, 2$ . Where we define the frequency detuning

$$\delta = \Delta_a - \Delta = \omega_a - \Omega, \quad (31)$$

and the parameter  $\Gamma$  is given by

$$\Gamma = \frac{\kappa}{2} + \frac{\gamma}{4}. \quad (32)$$

The parameters  $\lambda_m$  can be further expressed as,  $\lambda_m = \Gamma_m + i\varphi_m$ , with real part

$$\Gamma_m = \Gamma + \frac{1}{2}(-1)^m(a^2 + b^2)^{\frac{1}{4}} \sin \left[ \frac{1}{2} \arctan \left( \frac{b}{a} \right) \right],$$

and imaginary part

$$\varphi_m = \frac{1}{2} \left\{ (-1)^m(a^2 + b^2)^{\frac{1}{4}} \cos \left[ \frac{1}{2} \arctan \left( \frac{b}{a} \right) \right] - (\Delta_a + \Delta) \right\}.$$

Here, the parameters  $a$  and  $b$  are

$$\begin{aligned} a &= \delta^2 - \left(\kappa - \frac{\gamma}{2}\right)^2 + 4g^2, \\ b &= 2\delta \left(\kappa - \frac{\gamma}{2}\right). \end{aligned}$$

### B. Correlation spectrum

The correlation function, e.g.,  $\langle a^\dagger(0)a(\tau) \rangle$ , is given by

$$\langle a^\dagger(0)a(\tau) \rangle = \text{Tr} \{a(0)A(\tau)\} \quad (33)$$

with

$$A(\tau) = U(\tau)\rho(0)a^\dagger(0)U^\dagger(\tau). \quad (34)$$

Using the quantum regression theorem<sup>35</sup>, the correlation function in Eq. (33) can be written as

$$\langle a^\dagger(0)a(\tau) \rangle = A_{01,00}(\tau), \quad (35)$$

with

$$A_{01,00}(\tau) = H_{A,12}^* e^{-\lambda_1^* \tau} + H_{A,21}^* e^{-\lambda_2^* \tau} + \varepsilon^*. \quad (36)$$

Here, the initial operator  $A(0)$  is assumed to be

$$A(0) = \rho^{ss} a^\dagger(0) \quad (37)$$

when we calculate the time-dependent matrix element  $A_{01,00}(\tau)$  in Eq. (36). The “ $ss$ ” in the superscript of the reduced density matrix  $\rho$  denotes the “steady state”. The parameters  $H_{A,12}$  and  $H_{A,21}$  in Eq. (36) are expressed as

$$H_{A,mn} = \mu_{mn}^* A_{01,00}(0) + \chi_{mn}^* A_{10,00}(0) - i\xi \nu_{mn}^*, \quad (38)$$

with the subscript either  $mn = 12$  or  $mn = 21$ . The parameters  $A_{00,01}(0)$  and  $A_{00,10}(0)$  denote the matrix elements of the operator  $A(0)$  in the truncated basis defined in Eq. (25), e.g.,

$$A_{00,01}(0) = \langle 00|A(0)|01 \rangle = \langle 00|\rho^{ss} a^\dagger(0)|01 \rangle. \quad (39)$$

These matrix elements  $A_{01,00}(0)$  and  $A_{10,00}(0)$  can be straightforwardly obtained as

$$A_{01,00}(0) = \rho_{01,01}^{ss}, \quad (40)$$

$$A_{10,00}(0) = \rho_{10,01}^{ss}, \quad (41)$$

where  $\rho_{01,01}^{ss}$  and  $\rho_{10,01}^{ss}$  denote the “steady-state” matrix elements of the reduced density matrix  $\rho$ .

Using the same procedure, other correlation functions can also be obtained as

$$\langle a(0)a^\dagger(\tau) \rangle = \text{Tr} \{a^\dagger(0)B(\tau)\} = B_{00,01}(\tau), \quad (42)$$

$$\langle a(0)a(\tau) \rangle = \text{Tr} \{a(0)C(\tau)\} = C_{01,00}(\tau), \quad (43)$$

$$\langle a^\dagger(0)a^\dagger(\tau) \rangle = \text{Tr} \{a^\dagger(0)D(\tau)\} = D_{00,01}(\tau), \quad (44)$$

with

$$B(\tau) = U(\tau)\rho(0)a(0)U^\dagger(\tau), \quad (45)$$

$$C(\tau) = U(\tau)\rho(0)a(0)U^\dagger(\tau), \quad (46)$$

$$D(\tau) = U(\tau)\rho(0)a^\dagger(0)U^\dagger(\tau), \quad (47)$$

and

$$B_{00,01}(\tau) = H_{B,12} e^{-\lambda_1 \tau} + H_{B,21} e^{-\lambda_2 \tau} + \varepsilon, \quad (48)$$

$$C_{01,00}(\tau) = H_{C,12}^* e^{-\lambda_1^* \tau} + H_{C,21}^* e^{-\lambda_2^* \tau} + \varepsilon^*, \quad (49)$$

$$D_{00,01}(\tau) = H_{D,12} e^{-\lambda_1 \tau} + H_{D,21} e^{-\lambda_2 \tau} + \varepsilon. \quad (50)$$

Here, the parameters  $H_{B,mn}$ ,  $H_{C,mn}$ , and  $H_{D,mn}$  are

$$H_{C,mn} = \mu_{mn}^* C_{01,00}(0) + \chi_{mn}^* C_{10,00}(0) - i\xi \nu_{mn}^*, \quad (51)$$

and

$$H_{X,mn} = \mu_{mn} X_{00,01}(0) + \chi_{mn} X_{00,10}(0) + i\xi \nu_{mn}. \quad (52)$$

Here, the subscript  $X$  can be either  $B$  or  $D$ . With the same meaning as in Eq. (39), the parameters, e.g.,  $C_{01,00}(0)$ , represent the matrix elements of the operators  $C(0)$ ,  $B(0)$ , and  $D(0)$  in the truncated basis in Eq. (25). We note that the initial conditions

$$B(0) = C(0) = \rho^{ss} a(0), \quad (53)$$

$$D(0) = A(0) = \rho^{ss} a^\dagger(0) \quad (54)$$

are used when Eqs. (42–44) are derived. The matrix elements, e.g.,  $B_{00,01}(0)$ , can also be obtained as

$$B_{00,01}(0) = \rho_{00,00}^{ss}, \quad (55)$$

using the quantum regression theorem with the matrix element  $\rho_{00,00}^{ss}$  of the reduced density matrix  $\rho$ .

By using Eq. (36) and Eqs. (42–44), the two-time correlation function in Eq. (22) for the induced electromotive force is given by

$$\begin{aligned} \langle V(0)V(\tau) \rangle &\propto A_{01,00}(\tau) + B_{00,01}(\tau) \\ &\quad - C_{01,00}(\tau) - D_{00,01}(\tau). \end{aligned} \quad (56)$$

Based on the above results, the two-time correlation function in Eq. (56) is further simplified to

$$\begin{aligned} \langle V(0)V(\tau) \rangle &\propto \mu_{12} e^{-\lambda_1 \tau} + \mu_{21} e^{-\lambda_2 \tau} \\ &\quad + f_1 e^{-\lambda_1^* \tau} + f_2 e^{-\lambda_2^* \tau} \end{aligned} \quad (57)$$

with

$$f_1 = \mu_{12}^* \rho_{01,01}^{ss} + \chi_{12}^* \rho_{10,01}^{ss},$$

$$f_2 = \mu_{21}^* \rho_{01,01}^{ss} + \chi_{21}^* \rho_{10,01}^{ss}.$$

Then, replacing  $\langle V(0)V(\tau) \rangle$  in Eq. (21) by Eq. (57), and integrating, the spectrum  $S_V(\omega)$  in Eq. (21) can be expressed as

$$\begin{aligned} S_V(\omega) &\approx \frac{B^2 l^2 \Omega}{2M} \text{Re} \left[ \int_0^\infty d\tau e^{i\omega\tau} (\mu_{12} e^{-\lambda_1 \tau} + \mu_{21} e^{-\lambda_2 \tau}) \right] \\ &= \frac{B^2 l^2 \Omega}{2M} \frac{\Gamma_1 \text{Re}(\mu_{12}) - (\omega - \varphi_1) \text{Im}(\mu_{12})}{(\omega - \varphi_1)^2 + \Gamma_1^2} \\ &\quad + \frac{B^2 l^2 \Omega}{2M} \frac{\Gamma_2 \text{Re}(\mu_{21}) - (\omega - \varphi_2) \text{Im}(\mu_{21})}{(\omega - \varphi_2)^2 + \Gamma_2^2}. \end{aligned} \quad (58)$$

In Eq. (58), we have neglected the terms proportional to the amplitudes  $f_1$  and  $f_2$ . This is because the ratios, e.g.,  $(f_1/\mu_{12})$ , are proportional to  $\xi^2$ , which is negligibly small in the weak driving limit. In this case, we need only consider the two leading terms, which are proportional to  $\mu_{12}$  and  $\mu_{21}$ , as shown in Eq. (58).

As shown in Figs. 2, 3, 4, there are two dominant peaks in the  $S_V(\omega)$  spectrum. The distance (splitting frequency  $\Delta\omega$ ) between these two peaks is

$$\Delta\omega = (a^2 + b^2)^{\frac{1}{4}} \cos \left[ \frac{1}{2} \arctan \left( \frac{b}{a} \right) \right], \quad (59)$$

which is determined by the frequency detuning  $\delta$  and the decay rates  $\kappa$  and  $\gamma$  for the NAMR and the charge qubit. Then, the information of the coherent coupling between the charge qubit and the NAMR can be obtained by Eq. (59).

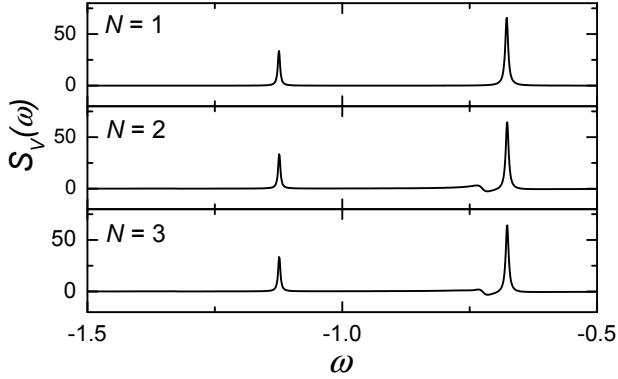


FIG. 2: The spectrum  $S_V(\omega)$  versus  $\omega$  for three different values of the total number of excitations  $N$ , e.g.,  $N = 1, 2, 3$ . We take the values for other parameters as  $\delta = 0.2$ ,  $g = 0.2$ ,  $\xi = 0.02$ ,  $\kappa = 0.004$  and  $\gamma = 0.004$ . Here, all these parameters are in units of 1 GHz.

### C. Numerical results

To test the validity of our analytical calculations obtained using both quantum regression theorem and perturbation theory, we now study the correlation spectrum  $S_V(\omega)$  numerically.

In Fig. 2, the spectrum  $S_V(\omega)$  versus frequency  $\omega$  is plotted with parameters  $\delta = 0.2$ ,  $g = 0.2$ ,  $\xi = 0.02$ ,  $\kappa = 0.004$ , and  $\gamma = 0.004$ , for different total excitation numbers  $N$ , e.g.,  $N = 1, 2, 3$ . Here, we take 1 GHz as the unit for all these parameters.

Figure 2 shows that: (i) there are two prominent peaks, which means that the approximation in Eq. (58) is valid in the weak driving limit; (ii) the increase of the total number  $N$  of the excitation does not obviously change the heights and the splitting frequency  $\Delta\omega$  of the two leading peaks. Therefore, Fig. 2 verifies that the approximation

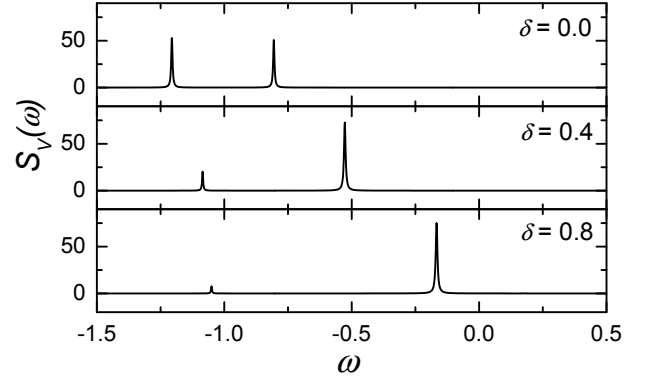


FIG. 3: The spectrum  $S_V(\omega)$  versus  $\omega$  for three different values of the detuning  $\delta$ , e.g.,  $\delta = 0, 0.4, 0.8$ . The detuning  $\delta$  is defined in Eq. (31). The total excitation number  $N$  is taken here as  $N = 1$ . Other parameters and units are the same as in Fig. 2.

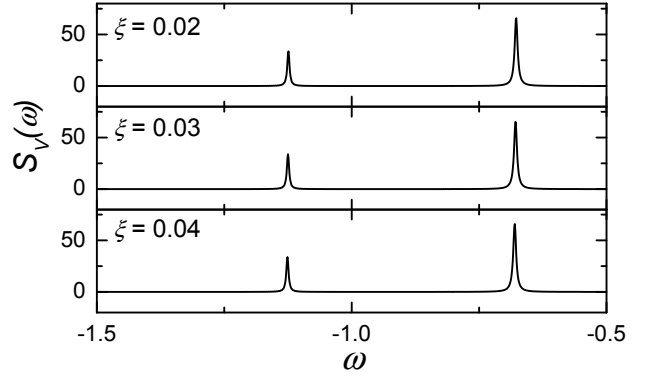


FIG. 4: The spectrum  $S_V(\omega)$  versus  $\omega$  for three different values of the driving strength  $\xi$ , e.g.,  $\xi = 0.02, 0.03, 0.04$ . The coupling strength  $\xi \equiv \xi_{\text{NAMR-current}}$  is defined in Eq. (19). The total excitation number  $N$  is taken here as  $N = 1$ . Other parameters and units are the same as in Fig. 2.

with the truncated basis ( $N = 1$ ) is valid in the limit of weak driving ( $\xi \ll g$ ).

Now in the truncated basis ( $N = 1$ ), let us demonstrate the effects of the frequency detuning  $\delta$  [see Eq. (31)] and the driving strength  $\xi$  [see Eq. (19)] on the splitting frequency  $\Delta\omega$ . In Fig. 3, the spectrum  $S_V(\omega)$  versus frequency  $\omega$  is plotted for different detunings  $\delta$ , and the same other parameters as in Fig. 2. Figure 3 shows that the detuning  $\delta$  affects both the heights and the frequency splitting  $\Delta\omega$  of the two peaks. A larger  $\delta$  corresponds to a larger frequency splitting  $\Delta\omega$ . When  $\delta$  is increased, the heights of the two peaks change *asymmetrically*, i.e., one peak becomes higher than another one when increasing the detuning  $\delta$ . (Similar results were found in Ref.<sup>34</sup>). This means that our probing approach does not work well when the frequency detuning ( $\delta = 0.8$ ) is much larger than the interaction strength ( $g = 0.2$ ). In practice, we

should assume that the frequency detuning  $\delta$  and the interaction strength  $g$  is of the same order. Also, Fig. 3 shows that the detuning  $\delta$  does not affect the number of peaks, which means that the approximation in Eq. (58) is valid in the weak driving limit.

Similarly, in Fig. 4, the spectrum  $S_V(\omega)$  versus frequency  $\omega$  is plotted for different driving strengths  $\xi$  and the same other parameters as in Fig. 2, when the total excitation number  $N = 1$ . Figure 4 shows that a weak driving strength  $\xi$  does not significantly affect the frequency splitting  $\Delta\omega$  of the two peaks, and also it does not affect the number of peaks. Moreover, changing the driving strength  $\xi$  does not affect the heights of both peaks.

#### IV. CONCLUSIONS

We have proposed an “intrinsic probing” approach to demonstrate the coherent coupling between a driven metallic NAMR and a charge qubit. This metallic NAMR can act as an intrinsic detector when a weak driving current passes through it. Using the quantum regression theorem and perturbation theory, we have calculated the correlation spectrum of the electromotive force between two ends of the NAMR. This spectrum can be used to demonstrate QED analogues in the NAMR-qubit system,

e.g., the vacuum Rabi splitting related to the coherent coupling strength of the charge qubit to the NAMR. The numerical calculations confirm the validity of the analytical results.

In our proposal, no additional measurement instruments need to be integrated, in contrast to the proposal in<sup>34</sup>. The NAMR acts as both the cavity and the detector. Therefore, it is easier to be fabricated. Our proposal can also be generalized to the case where many qubits are coupled to a NAMR. In this case, the information of many qubits can also be readout via the spectrum of the electromotive force. Recent experiments<sup>33</sup> indicate that our proposal is experimentally realizable.

#### Acknowledgments

We acknowledge the support of the NSFC Grant Nos. 10547101, 10604002, the National Fundamental Research Program of China Grant No. 2006CB921200. FN acknowledges partial support from the National Security Agency (NSA), Laboratory Physical Science (LPS), Army Research Office (ARO), National Science Foundation (NSF) grant No. EIA-0130383, JSPS-RFBR 06-02-91200, and Core-to-Core (CTC) program supported by the Japan Society for Promotion of Science (JSPS). We also thank N. Zhao for discussions.

- 
- \* Electronic address: ybgao@bjut.edu.cn
- <sup>1</sup> A. N. Cleland, *Foundations of Nanomechanics: From Solid-State Theory to Device Applications* (Springer-Verlag, Berlin, 2002).
  - <sup>2</sup> M. P. Blencowe, Phys. Rep. **395**, 159 (2004).
  - <sup>3</sup> M. P. Blencowe and E. Buks, Phys. Rev. B **76**, 014511 (2007); E. Buks, S. Zaitsev, E. Segev, B. Abdo, and M. P. Blencowe, Phys. Rev. E **76**, 026217 (2007).
  - <sup>4</sup> I. Mahboob and H. Yamaguchi, Nature Nanotech. **3**, 275 (2008).
  - <sup>5</sup> A. D. Armour, M. P. Blencowe, and K. C. Schwab, Phys. Rev. Lett. **88**, 148301 (2002).
  - <sup>6</sup> E. K. Irish and K. C. Schwab, Phys. Rev. B **68**, 155311 (2003).
  - <sup>7</sup> A. N. Cleland and M. R. Geller, Phys. Rev. Lett. **93**, 070501 (2004).
  - <sup>8</sup> S. Savel'ev, A. L. Rakhmanov, X. Hu, A. Kasumov, and F. Nori, Phys. Rev. B **75**, 165417 (2007).
  - <sup>9</sup> Y. D. Wang, Y. B. Gao, and C. P. Sun, Eur. J. Phys. B **40**, 321 (2004).
  - <sup>10</sup> F. Xue, Y. X. Liu, C. P. Sun, and F. Nori, Phys. Rev. B **76**, 064305 (2007).
  - <sup>11</sup> F. Xue, Y. D. Wang, C. P. Sun, H. Okamoto, H. Yamaguchi, and K. Semba, New J. Phys. **9**, 35 (2007); F. Xue, L. Zhong, Y. Li, and C. P. Sun, Phys. Rev. B **75**, 033407 (2007).
  - <sup>12</sup> I. Martin, A. Shnirman, L. Tian, and P. Zoller, Phys. Rev. B **69**, 125339 (2004).
  - <sup>13</sup> P. Zhang, Y. D. Wang, and C. P. Sun, Phys. Rev. Lett. **95**, 097204 (2005).
  - <sup>14</sup> A. Naik, O. Buu, M. D. LaHaye, A. D. Armour, A. A. Clerk, M. P. Blencowe, and K. C. Schwab, Nature **443**, 193 (2006).
  - <sup>15</sup> M. Grajcar, S. Ashhab, J. R. Johansson, and F. Nori, Phys. Rev. B **78**, 035406 (2008).
  - <sup>16</sup> F. Xue, Y. D. Wang, Y. X. Liu, and F. Nori, Phys. Rev. B **76**, 205302 (2007); Y. D. Wang, K. Semba, and H. Yamaguchi, New J. Phys. **10**, 043015 (2008); Y. Li, Y. D. Wang, F. Xue, and C. Bruder, Phys. Rev. B **78**, 134301 (2008).
  - <sup>17</sup> Y. Makhlin, G. Schön, and A. Shnirman, Rev. Mod. Phys. **73**, 357 (2001).
  - <sup>18</sup> J. Q. You and F. Nori, Phys. Today **58** (11), 42 (2005).
  - <sup>19</sup> G. Wendin and V. S. Shumeiko, in *Handbook of Theoretical and Computational Nanotechnology*, edited by M. Rieth and W. Schommers (ASP, Los Angeles, 2006).
  - <sup>20</sup> J. Clarke and F. K. Wilhelm, Nature **453**, 1031 (2008).
  - <sup>21</sup> N. Lambert and F. Nori, Phys. Rev. B **78**, 214302 (2008).
  - <sup>22</sup> S. H. Ouyang, J. Q. You, and F. Nori, arXiv:0807.4833 (Phys. Rev. B, in press).
  - <sup>23</sup> J. R. Johansson, L. G. Mourokh, A. Yu. Smirnov, and F. Nori, Phys. Rev. B **77**, 035428 (2008).
  - <sup>24</sup> A. Shnirman and G. Schön, Phys. Rev. B **57**, 15400 (1998).
  - <sup>25</sup> J. Q. You, J. S. Tsai, and F. Nori, Phys. Rev. B **68**, 024510 (2003); J. Q. You and F. Nori, Phys. Rev. B **68**, 064509 (2003).
  - <sup>26</sup> Y. X. Liu, L. F. Wei, and F. Nori, Europhys. Lett. **67**, 941 (2004); Phys. Rev. A **71**, 063820 (2005).
  - <sup>27</sup> A. Wallraff, D. I. Schuster, A. Blais, L. Frunzio, R. S. Huang, J. Majer, S. Kumar, S. M. Girvin, and R. J.

- Schoelkopf, Nature **431**, 162 (2004).
- <sup>28</sup> J. E. Mooij, T. P. Orlando, L. Levitov, L. Tian, C. H. van der Wal, and S. Lloyd, Science **285**, 1036 (1999).
- <sup>29</sup> E. Il'ichev, N. Oukhanski, A. Izmailkov, Th. Wagner, M. Grajcar, H. G. Meyer, A. Yu. Smirnov, A. Maassen van den Brink, M. H. S. Amin, and A. M. Zagoskin, Phys. Rev. Lett. **91**, 097906 (2003).
- <sup>30</sup> J. Hauss, A. Fedorov, C. Hutter, A. Shnirman, and G. Schön, Phys. Rev. Lett. **100**, 037003 (2008); J. Q. You, Y. X. Liu, and F. Nori, Phys. Rev. Lett. **100**, 047001 (2008).
- <sup>31</sup> J. M. Raimond, M. Brune, and S. Haroche, Rev. Mod. Phys. **73**, 565 (2001).
- <sup>32</sup> R. J. Schoelkopf and S. M. Girvin, Nature **451**, 664 (2008).
- <sup>33</sup> T. F. Li, Yu. A. Pashkin, O. Astafiev, Y. Nakamura, J. S. Tsai, and H. Im, Appl. Phys. Lett. **92**, 043112 (2008).
- <sup>34</sup> L. F. Wei, Y. X. Liu, C. P. Sun, and F. Nori, Phys. Rev. Lett. **97**, 237201 (2006).
- <sup>35</sup> M. O. Scully and M. S. Zubairy, *Quantum Optics* (Cambridge University Press, Cambridge, 1997).
- <sup>36</sup> Y. Makhlin, G. Schön, and A. Shnirman, Nature **386**, 305 (1999).
- <sup>37</sup> H. J. Carmichael, *Statistical Methods in Quantum Optics 1: Master Equations and Fokker-Planck Equations* (Springer, Berlin, 1999).